

Orientation Tuning of a Polypyridyl Ru(II) Complex Immobilized on a Clay Surface toward Chiral Discrimination

Hisako Sato,^{*,†,§} Yoshihisa Hiroe,[†] Kenji Tamura,[‡] and Akihiko Yamagishi^{†,§}

Department of Earth and Planetary Science, Graduate School of Science, The University of Tokyo, Tokyo 113-0033, Japan, and Ecomaterials Center, National Institute for Materials Science, 1-1 Namiki, Tsukuba, Ibaraki 305-0044, Japan

Received: June 29, 2005; In Final Form: July 29, 2005

The present work reports an attempt to elucidate a stereoselective energy-transfer system by immobilizing a chiral metal complex on a clay surface. The metal complex used was $[\text{Ru}(\text{bpy})_2\text{L}_i]^{2+}$ with $\text{L}_1 = \text{bpy}$ (2,2'-bipyridine), $\text{L}_2 = 4,4'$ -diundecyl-2,2'-bipyridine, and $\text{L}_3 = 5,5'$ -diundecyl-2,2'-bipyridine. The adsorption structure of $[\text{Ru}(\text{bpy})_2\text{L}_i]^{2+}$ was studied by means of electric dichroism measurements on an aqueous dispersion of a colloidal clay. It was found that the molecular orientation of the adsorbed Ru(II) complex was affected remarkably by the positions of the alkyl chains on the bpy ligand; that is, the angle of the 3-fold or pseudo-3-fold symmetry axis of the Ru(II) complex with respect to the surface normal was obtained to be 24°, 30°, and 52° for $i = 1, 2$, and 3, respectively. The efficiency of the energy-transfer was determined by photoluminescence quenching measurements between the adsorbed Ru(II) complex and $[\text{Ru}(\text{acac})_3]$ (acac = acetylacetonate) in solution. As a result, stereoselectivity appeared most for the case of $[\text{Ru}(\text{bpy})_2\text{L}_3]^{2+}$ in which its two helically twisted bpy ligands were projected in an outward direction.

Introduction

Chemical reactions on the surface of an inorganic layered material have been of great interest for their potential application as catalysts, photochemical reactions, and molecular devices.^{1–16} Thin inorganic layers (often called nanosheets) are obtained by exfoliating layered inorganic compounds as a colloidal dispersion.^{14,15} Among such layered inorganic materials, a clay mineral takes a unique position because of its network surface structure together with cation-exchange properties.^{3–12} When a cationic molecule is adsorbed by a clay, it may exist at high density under steric control by phyllosilicate surfaces.¹⁰

One such effect is the possibility of a stereoselective interaction between an adsorbed molecule and its neighbors on a clay surface.^{5–9} That is, an optically active molecule may experience intermolecular interaction with its neighbors, depending on their molecular chirality.^{16–19} In fact, the present authors have reported evidence that a certain kind of metal complex prefers to form a racemic pair rather than an enantiomeric pair when it is adsorbed by colloiddally dispersed sodium montmorillonite.⁵ To understand the origin of such chirality effects, we have made theoretical calculations of the adsorption states of metal complexes on clay.¹⁷ As a result, chiral discrimination ability is enhanced among uniformly oriented molecules. Such an orientation is achieved because of the geometrical matching between a phyllosilicate network and a bulky metal complex with C_3 symmetry such as $[\text{M}(\text{bpy})_3]^{2+}$ (bpy = 2,2'-bipyridine) or $[\text{M}(\text{phen})_3]^{2+}$ (phen = 1,10-phenanthroline).^{18–19}

In this paper, we report the orientation effects of adsorbed polypyridyl Ru(II) complexes on their chiral discrimination in an energy-transfer reaction. The orientation of the metal complex

was varied by attaching alkyl chains to the different positions of a bpy ligand. The photochemical energy transfer between polypyridyl Ru(II) complexes and chiral $[\text{Ru}(\text{acac})_3]$ (acac = acetylacetonate) in a solution as a quencher was examined by the phosphorescence measurements. As a result, the efficiency of chiral discrimination was found to be affected by tuning the orientation of an adsorbed molecule on a clay surface.

Experimental Section

Syntheses of Amphiphilic Ruthenium(II) Complexes. The metal complex used was $[\text{Ru}(\text{bpy})_2\text{L}_i]^{2+}$ with $\text{L}_1 = \text{bpy}$ (2,2'-bipyridine), $\text{L}_2 = 4,4'$ -diundecyl-2,2'-bipyridine, and $\text{L}_3 = 5,5'$ -diundecyl-2,2'-bipyridine. $[\text{Ru}(\text{bpy})_2\text{L}_1]^{2+}$ was purchased (Aldrich Chem.) and resolved according to the reported method.²⁰ The method of syntheses of amphiphilic ligands was described in a previous paper.²⁰ In the case of L_2 , for example, a solution of 4,4'-dimethyl-2,2'-bipyridyl (1.00 g, 5.42 mmol; Wako Chem. Ind., Japan) in dry THF (30 cm³) was cooled to below −40 °C under nitrogen, and a large excess of lithium diisopropylamide (LDA) (1.52 mL, 10.84 mmol) was added slowly over a time period of more than 30 min. After stirring at −40 °C for 3 h, we added a large excess of undecylbromide (6.50 mmol) in dry THF (20 cm³). The reaction mixture was slowly warmed to room temperature while stirring overnight. The mixture was quenched with water (1–2 cm³), and the solvent was removed in vacuo. All of the compounds were recrystallized in ethanol several times: 4,4'-diundecyl-2,2'-bipyridine (L_2). Yield 58%, (200 MHz, CDCl_3/TMS , δ): 0.88 (t, 6H, bpy- CH_2 -C₉-CH₃), 1.25 (36H, bpy- CH_2 -C₉-(CH₂)₉-CH₃), 2.69 (t, 4H, bpy-CH₂-C₉-CH₃), 7.13 (d, 2H, bpy-5,5'), 8.22 (s, 2H, bpy-3,3'), 8.55 (d, 2H, bpy-6,6'); 5,5'-diundecyl-2,2'-bipyridine (L_3). Yield 48%, (200 MHz, CDCl_3/TMS , δ): 0.88 (t, 6H, bpy-CH₂-C₉-CH₃), 1.28 (36H, bpy-CH₂-C₉-(CH₂)₉-CH₃), 2.65 (t, 4H, bpy-CH₂-C₉-CH₃), 7.60 (d, 2H, bpy-3,3'), 8.26 (d, 2H, bpy-3,3'), 8.48 (s, 2H, bpy-6,6').

The chloride salt of $[\text{Ru}(\text{bpy})_2\text{L}_1]^{2+}$ was purchased from Aldrich Chem. The complex was resolved by use of sodium

* Corresponding author. Phone: +81-03-5841-4553; e-mail: h-sato@eps.s.u-tokyo.ac.jp.

[†] The University of Tokyo.

[‡] National Institute for Materials Science.

[§] Also at: CREST, Japan Science and Technology Agency.

antimonyl tartrate ($\text{Na}_2(\text{SbOtar})_2$) as described previously.^{5b} The chloride salts of $[\text{Ru}(\text{bpy})_2\text{L}_2]^{2+}$ and $[\text{Ru}(\text{bpy})_2\text{L}_3]^{2+}$ were prepared by refluxing $[\text{Ru}(\text{bpy})_2\text{Cl}_2]$ (Aldrich Chem.) with the ligands (L_2 and L_3) in ethanol. The products were attempted to be resolved similarly by use of $\text{Na}_2(\text{SbOtar})_2$ as a resolving agent.²⁰ For both $[\text{Ru}(\text{bpy})_2\text{L}_2]^{2+}$ and $[\text{Ru}(\text{bpy})_2\text{L}_3]^{2+}$, the Λ -isomers formed insoluble salts with $(\text{SbOtar})_2^{2+}$ in a 1:3 (v/v) methanol/water solution. The perchlorate salts of chiral Ru(II) complexes were obtained by the use of ion-exchanged resin. The compounds were further purified by HPLC on a reversed phase column (CAPCELL PAK Shiseido Co., Ltd. (Japan)) with a water–methanol solvent. The Λ -isomers of $[\text{Ru}(\text{bpy})_2\text{L}_i](\text{ClO}_4)_2$ gave nearly the same values of $\Delta\epsilon$ at 290 nm = 290 ± 3 for $i = 1-3$. The Δ isomers were, however, unable to be purified sufficiently so that they attained at most -150 to -200 as $\Delta\epsilon$ at 290 nm for all three complexes. Thus, the experiments investigating the chirality effect were performed by using racemic mixtures and Λ -isomers.

Clays. Sodium montmorillonite (Na-Mont) was purchased from Kunimine Ind. Co. (Japan) (Kunipia F), whose elemental composition was stated to be $[(\text{Si}_{7.70}\text{Al}_{0.30})(\text{Al}_{3.12}\text{Mg}_{0.68}\text{Fe}_{0.19})\text{O}_{20}(\text{OH})_4](\text{Na}_{0.49}\text{Mg}_{0.14})$ with the cation-exchange capacity (CEC) of 115 meq/100 g.

Adsorption Experiments. The above clay sample was dispersed by being stirred for 1 day in distilled water and adjusted to 1.00 g L^{-1} . Adsorption experiments were performed by adding a $100 \mu\text{L}$ of a clay stock solution (1.15×10^{-3} equivalent L^{-1} in CEC) to 1.5 mL of 1:1 (v/v) methanol/water containing various amounts of metal complex (1×10^{-5} to $3 \times 10^{-4} \text{ M}$). To adjust the ionic strength, we added 0.1 M of Na_2SO_4 . The mixture was left overnight and centrifuged at $10\,000 \text{ rms}$ for 1 h. The equilibrium concentration of the metal complex was determined from the UV–vis absorption spectrum of the supernatant solution (ϵ at $450 \text{ nm} = 14\,800$ for the three types of complexes).

The change of enantiomeric excess (ee) on the progress of adsorption by a clay was investigated by adding various amounts of clay (0.0 to $1.0 \times 10^{-4} \text{ g}$) to 1.5 mL of 1:1 (v/v) methanol/water, which contained a partially resolved metal complex ($1 \times 10^{-4} \text{ M}$). The initial ratio of Δ -isomer to Λ -isomer was taken to be ca. 1:3. The mixture was left overnight and centrifuged at $10\,000 \text{ rms}$ for 1 h. The optical purity of the supernatant solution was determined from the circular dichroism spectra, assuming that $\Delta\epsilon$ at $290 \text{ nm} = +250$ or -250 for the pure Λ - or Δ -isomers for the three types of complexes.

Instruments. The orientation of a metal complex adsorbed by a colloidal clay particle was studied by means of electric dichroism measurements. The apparatus consisted of an optical system, a pulse generator, a light detector, and a signal processing system.^{21–23} A monitoring light emitted from a 150-W xenon lamp power supply (Hamamatsu, Japan) was monochromatized through a monochromator. A rotatable polarizer (Glan-Thompson polarizer) was placed between a cell and a photomultiplier. A quartz cell contained two gold-coated electrodes with a distance of 0.4 mm and an optical length of 1.0 cm . An electric field pulse of $1.0 \text{ ms} \times 0.5\text{--}2.0 \text{ kVcm}^{-1}$ was applied with a high voltage pulse generator model-60320 (Denkenseiki, Japan). The transient change of transmittance was monitored and stored into a transient oscilloscope (TDS1012 Digital Oscilloscope, Tektronix). The angle ϕ of the polarization of a monitoring light with respect to an electric field is related to the observed absorbance change according to

$$\Delta A = \left(\frac{A}{3}\right)\left(\frac{\Delta\epsilon}{\epsilon}\right)(3 \cos^2 \phi - 1) \quad (1)$$

in which A , ΔA , ϵ , and $\Delta\epsilon$ denote the isotropic absorbance, the absorbance change induced by imposing an electric field pulse, the isotropic extinction coefficient, and the difference between parallel and vertical extinction coefficients ($\epsilon_p - \epsilon_v$), respectively.²⁴ The reduced linear dichroism, ρ , is defined by

$$\rho = \frac{\epsilon_p - \epsilon_v}{\epsilon} \quad (2)$$

with $\epsilon = (1/3)(\epsilon_p + 2\epsilon_v)$. The parameter, ρ , at complete orientation (denoted by ρ_0) is obtained by extrapolation to the infinite field strength. Here ρ_0 gives us a clue to the direction of a transition moment with respect to the oriented axis of a particle.²⁴ The adsorption of the metal complex, ρ_0 , is expressed as follows²³

$$\rho_0 = \frac{3}{8}(2 - 3 \sin^2 \theta) \quad (3)$$

Here θ is an angle between the C_3 or pseudo C_3 axis of the metal complex and the normal of the clay surface. The sample was prepared by mixing equal volumes of a 1:1 (v/v) methanol/water solution of a metal complex with a 1:1 (v/v) methanol/water suspension of a clay rapidly by use of a stopped-flow apparatus.^{21b} The final concentrations were adjusted to be $1 \times 10^{-4} \text{ M}$ clay (in CEC) and $0.75\text{--}2.0 \times 10^{-5} \text{ M}$ metal complex.

UV–vis absorption spectra were recorded on a Hitachi U-2810 spectrophotometer. CD spectra were measured with a JASCO J-720 spectropolarimeter. High-performance liquid chromatography (HPLC) was performed with a JASCO BIP-II chromatograph equipped with a JASCO UV-100 detector. The flow rate of methanol as an eluent was 0.5 mL min^{-1} under a pressure of 125 kg cm^{-2} . XRD measurements were performed with a RINT Ultima System using monochromatic $\text{Cu K}\alpha$ radiation.

Phosphorescence spectra were measured with a FP6500 spectrofluorometer (JASCO Co., Ltd., Japan). The phosphorescence intensity at 600 nm was measured at various concentrations of enantiomeric $[\text{Ru}(\text{acac})_3]$ (acac = acetyl acetonate; Aldrich Chem.) when a 1:2 (v/v) methanol/water dispersion of a clay/metal complex adduct was irradiated at 450 nm . The Δ - and Λ -isomers of $[\text{Ru}(\text{acac})_3]$ were obtained by the chromatographic resolution of the racemic mixture on a chiral column as described previously.^{5b}

Ab Initio Calculation of Molecular Structures. The sectional area of the molecule was estimated on the basis of the stable molecular structure determined by the ab initio calculation using the Gaussian 03 program.²⁵ In the calculation, $[\text{Ru}(\text{bpy})_2\text{L}_i]^{2+}$ ($i = 1-3$) was geometrically optimized at the Hartree–Fock level with the basis set of 6-31G(d). Here the central metal ion (Ru(II)) was replaced by Mg(II) on the basis of the assumption that the molecular structure was not affected greatly by the participation of d electrons.²⁰

Results

Adsorption Measurements. The possibility of stereoselective interaction among adsorbed molecules on a clay surface was investigated in two different ways. First, the adsorption isotherm was compared when the complex was added as either a pure enantiomer or a racemic mixture. Second, the optical purity of a partially resolved metal complex was measured by changing the amount of added clay. In the case of tris(1,10-phenanthroline)ruthenium(II) ($[\text{Ru}(\text{phen})_3]^{2+}$), its racemic mixture is reported to be absorbed to nearly two times the CEC, while its pure enantiomer is absorbed within the CEC.⁵ In addition, the

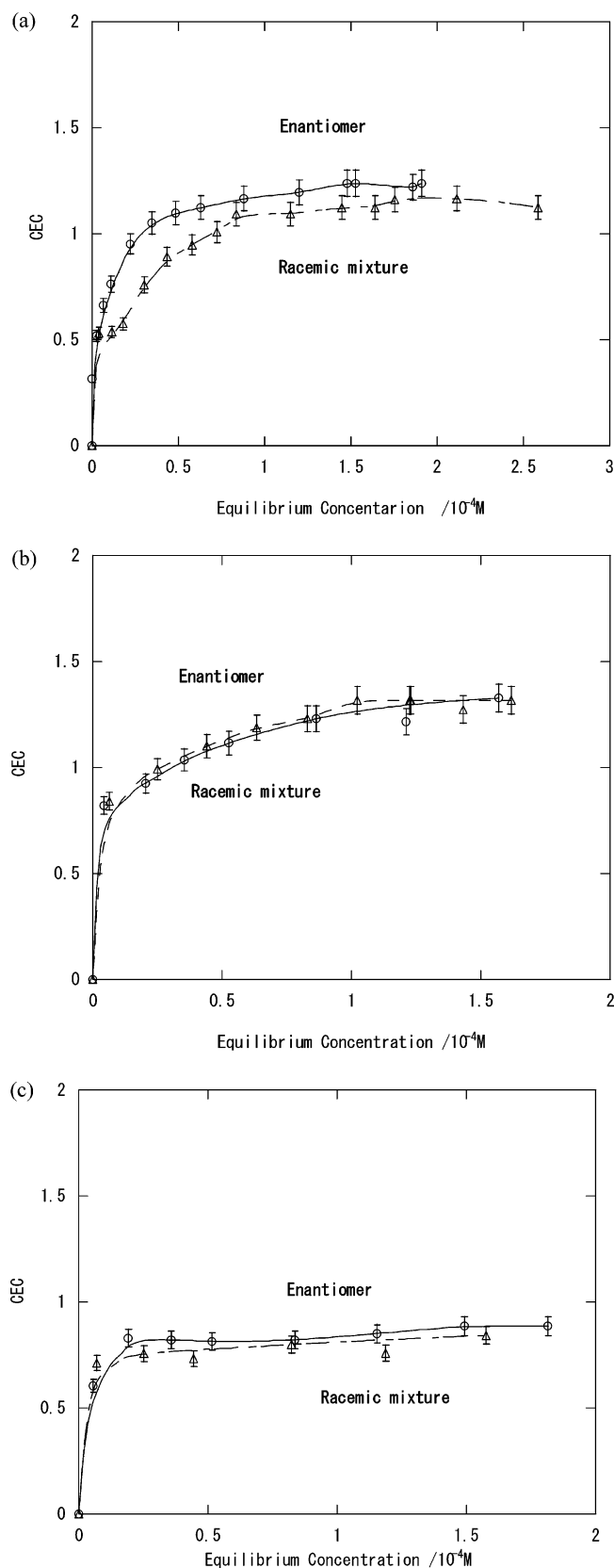


Figure 1. Adsorption isotherms of enantiomeric and racemic ruthenium(II) complexes by a clay: (a) $[\text{Ru}(\text{bpy})_2\text{L}_1]^{2+}$, (b) $[\text{Ru}(\text{bpy})_2\text{L}_2]^{2+}$, and (c) $[\text{Ru}(\text{bpy})_2\text{L}_3]^{2+}$.

optical purity of a partially resolved solution was found to increase on the progress of adsorption by a clay. The results indicated that this molecule has a tendency to be adsorbed as a racemic pair rather than as an enantiomeric pair.

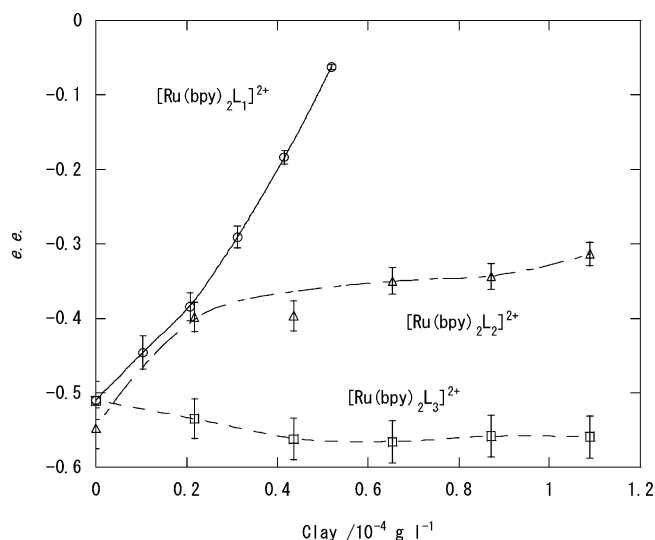


Figure 2. Dependence of ee on the amount of an added clay for three types of complexes.

Figure 1a–c shows the adsorption curves for the racemic mixtures and Λ -enantiomers for $[\text{Ru}(\text{bpy})_2\text{L}_i]^{2+}$ with $\text{L}_1 = \text{bpy}$ (2,2'-bipyridine), $\text{L}_2 = 4,4'$ -diundecyl-bipyridine, and $\text{L}_3 = 5,5'$ -diundecyl-bipyridine, respectively. For $[\text{Ru}(\text{bpy})_2\text{L}_1]^{2+}$, the racemic mixture was adsorbed nearly to the CEC of a clay, whereas the enantiomer was adsorbed to 1.2 times the CEC. The molecule was thus adsorbed with a tendency to prefer to the enantiomeric association on a clay surface.^{6,26} For $[\text{Ru}(\text{bpy})_2\text{L}_2]^{2+}$, no difference was observed in the maximum adsorption amount within experimental error. The maximum adsorption attained 1.3 times the CEC for both cases. For $[\text{Ru}(\text{bpy})_2\text{L}_3]^{2+}$, both the racemic mixture and the enantiomer were adsorbed in the same way until they attained the maximum adsorption level below 0.9 times of CEC. These results implied that the adsorption amount was not affected by the stereoselective interaction among the adsorbates for both $[\text{Ru}(\text{bpy})_2\text{L}_2]^{2+}$ and $[\text{Ru}(\text{bpy})_2\text{L}_3]^{2+}$.

The change of the Δ - to Λ -enantiomeric ratio was investigated by varying the adsorption amount of the clay. For that purpose, various amounts of clay were added to a solution containing a partially resolved metal complex. Figure 2 shows the plot of enantiomeric excess (ee) in a supernatant solution as a function of the added amount of clay, where ee was defined as

$$ee = \frac{\Delta - \Lambda}{\Delta + \Lambda} \quad (4)$$

For $[\text{Ru}(\text{bpy})_2\text{L}_1]^{2+}$ and $[\text{Ru}(\text{bpy})_2\text{L}_2]^{2+}$, the ee in supernatant solution decreased with the increase of added amount of clay. Corresponding to this, the composition of the supernatant approached that of a racemic mixture or zero ee. It implied that these chelates exhibited a tendency for enantiomeric pairing when they were adsorbed by clay. In contrast, no change of ee was observed for $[\text{Ru}(\text{bpy})_2\text{L}_3]^{2+}$, indicating that the enantiomeric composition of adsorbed molecules was identical to that in solution. In other words, Δ - and Λ -enantiomers were distributed randomly on the clay surface.

Electric Dichroism Measurements. On imposing an electric field pulse, the transient change of transmittance was observed in the wavelength region of 400–500 nm where the metal complex showed the MLCT (metal-to-ligand charge transfer) transition in the electronic absorption spectra. The signal amplitude in terms of absorbance change, ΔA , obeyed orientational dichroism as in eq 1 with no isotropic absorbance change

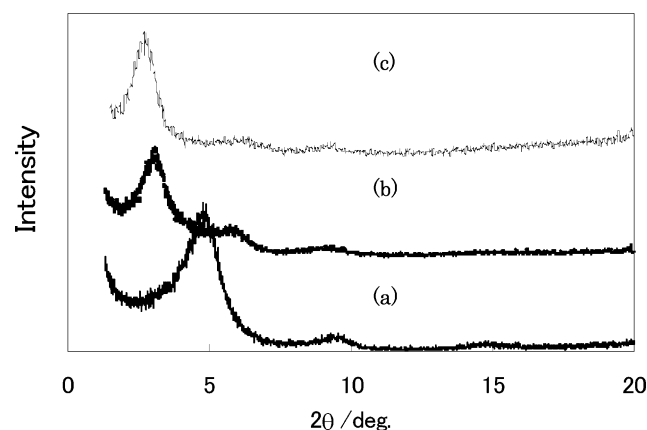


Figure 3. X-ray diffraction patterns for the ion-exchange adducts of $[\text{Ru}(\text{bpy})_2\text{L}_2]^{2+}$ and a clay. The loading of the metal complex was (a) 10% of CEC, (b) 50% of CEC, and (c) 100% of CEC. Three peaks were assigned to (001), (002), and (003) diffractions, respectively.

TABLE 1: Results of Electric Dichroism Measurements on Ruthenium(II) Complexes Adsorbed by a Clay

	metal complex	θ (deg) from C_3 (or pseudo- C_3 axis)	
		15% CEC	40% CEC
racemic mixture	$[\text{Ru}(\text{bpy})_2\text{L}_1]^{2+}$	23.6 ± 0.4	23.6 ± 0.4
	$[\text{Ru}(\text{bpy})_2\text{L}_2]^{2+}$	30.0 ± 0.5	33.3 ± 0.5
	$[\text{Ru}(\text{bpy})_2\text{L}_3]^{2+}$	52.7 ± 0.7	52.8 ± 0.7
enantiomer	$[\text{Ru}(\text{bpy})_2\text{L}_1]^{2+}$	24.2 ± 0.4	24.2 ± 0.4
	$[\text{Ru}(\text{bpy})_2\text{L}_2]^{2+}$	30.1 ± 0.5	32.5 ± 0.5
	$[\text{Ru}(\text{bpy})_2\text{L}_3]^{2+}$	52.4 ± 0.7	52.7 ± 0.7

induced by the electric field. The wavelength dependence of ΔA was coincident with the isotropic absorbance (denoted by A) in the wavelength range of 400–500 nm. The results indicated that these metal complexes behaved as a uniaxial molecule with the C_3 symmetry on a clay surface.²⁴ In other words, the adsorbed state was specified only by the orientation angle (θ) of the C_3 or pseudo C_3 axis with respect to the normal of a clay surface. The angle (θ) was determined from the reduced linear dichroism (ρ_o), which was obtained by extrapolating the linear dichroism to an infinite strength of electric field according to eq 3. Table 1 gives the orientation angle of the C_3 axis on a clay as determined by the electric measurements. At the loading of 15% CEC, θ was obtained to be 24° , 30° , and 52° for $[\text{Ru}(\text{bpy})_2\text{L}_1]^{2+}$, $[\text{Ru}(\text{bpy})_2\text{L}_2]^{2+}$, and $[\text{Ru}(\text{bpy})_2\text{L}_3]^{2+}$, respectively. The increase of the loading amount up to 40% CEC affected the orientation of an adsorbed chelate in a different way; that is, the value of θ was unaffected by the change of loading for $[\text{Ru}(\text{bpy})_2\text{L}_1]^{2+}$ and $[\text{Ru}(\text{bpy})_2\text{L}_3]^{2+}$, whereas θ increased for $[\text{Ru}(\text{bpy})_2\text{L}_2]^{2+}$. There was no difference in θ between a racemic mixture and an enantiomer at any loading. Thus, a metal complex with alkyl groups at the 4 and 4' positions at the coordinated bpy ligand underwent an orientation change with the increase of loading.

XRD Measurements. To investigate the intercalation structures of metal complexes in a layered clay, we performed XRD measurements on the solid adducts of clay and metal complexes. Figure 3 shows the X-ray diffraction patterns of the clay adducts with racemic $[\text{Ru}(\text{bpy})_2\text{L}_2]^{2+}$ at the loading of 10, 50, and 100% of CEC. The basal spacing increased from 1.85 to 3.25 nm with the increase of loading. The results indicated that the complex oriented more upright in an interlayer space with the increase of surface density. This was thought to be caused by the intermolecular interaction among the adsorbed molecules. Figure 4 shows the X-ray diffraction patterns of the clay adducts with

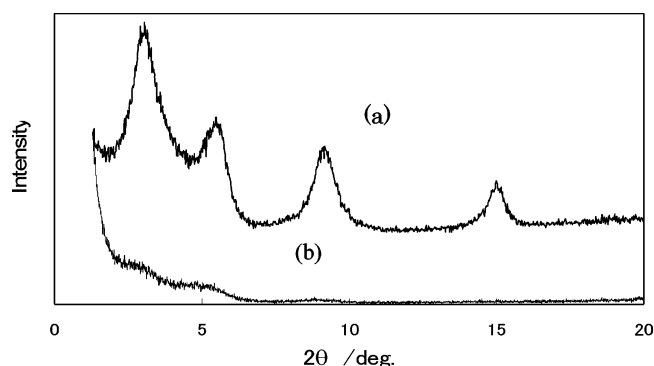


Figure 4. X-ray diffraction patterns for the ion-exchange adducts of metal complexes and a clay at the maximum loading (a) $[\text{Ru}(\text{bpy})_2\text{L}_1]^{2+}$ and (b) $[\text{Ru}(\text{bpy})_2\text{L}_3]^{2+}$. Four peaks in curve a were assigned to (001), (002), (003), and (004) diffractions, respectively. Three peaks in curve b were assigned to (001), (002), and (003) diffractions, respectively.

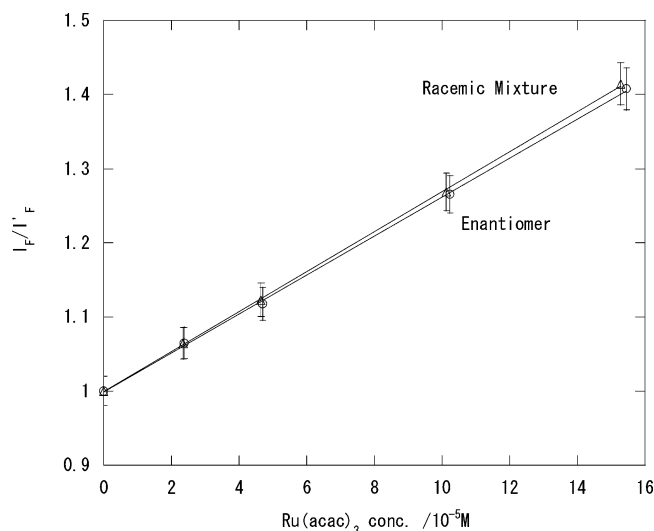


Figure 5. Stern–Volmer plots of the phosphorescence at 600 nm, quenched by either racemic or Δ - $[\text{Ru}(\text{acac})_3]$. The phosphorescence is due to racemic $[\text{Ru}(\text{bpy})_2\text{L}_2]^{2+}$ adsorbed by a clay. Various amounts of $[\text{Ru}(\text{acac})_3]$ were added to a 1:2 (v/v) methanol/water dispersion of ion-exchange adduct of $[\text{Ru}(\text{bpy})_2\text{L}_2]^{2+}$ (2.0×10^{-5} M) and a clay (1×10^{-4} M in CEC).

racemic $[\text{Ru}(\text{bpy})_2\text{L}_1]^{2+}$ and $[\text{Ru}(\text{bpy})_2\text{L}_3]^{2+}$ at the maximum loading. Although the broadening of the peaks occurred for $[\text{Ru}(\text{bpy})_2\text{L}_3]^{2+}$, both gave nearly the same basal spacing of 1.96 nm. No significant change of the basal spacing was observed for these complexes when the loading was lowered down to 10% (not shown). Thus, these complexes did not change orientation in an interlayer space for the change of surface density.

Phosphorescence Measurements. We examined the influence of orientation tuning on the reactivity of a metal complex adsorbed by a clay. For that purpose, the quenching rate of phosphorescence due to an adsorbed Ru(II) chelate was measured. The Δ - or Λ -enantiomer of $[\text{Ru}(\text{acac})_3]$ was dissolved as a quencher in a 1:2 (v/v) methanol/water mixture in which an adduct of a clay and a metal complex was dispersed. The clay adduct was formed with either a racemic mixture or an Λ -enantiomer of $[\text{Ru}(\text{bpy})_2\text{L}_i]^{2+}$ ($i = 1, 2$, and 3). The phosphorescence intensity ($\lambda_f = 600$ nm) due to an excited Ru(II) complex ($\lambda_{ex} = 450$ nm) was measured in the presence of various amounts of quencher.

Figure 5 shows the Stern–Volmer plots when the phosphorescence due to adsorbed racemic $[\text{Ru}(\text{bpy})_2\text{L}_2]^{2+}$ was quenched

TABLE 2: Quenching Rate of the Phosphorescence Due to a Ruthenium(II) Complex on a Clay by [Ru(acac)₃] in a 1:2 (v/v) Methanol/Water Solution

chelate	isomer	quencher [Ru(acac) ₃]	k_q/k_f (10 ³ M ⁻¹)		k_q/k_f (Λ/Λ)/ k_q/k_f (Λ/Δ)	
			10% CEC	40% CEC	10% CEC	40% CEC
[Ru(bpy) ₂ L ₁] ²⁺	racemic mixture	racemic mixture	2.89 ± 0.05	2.98 ± 0.05		
		Λ	2.67 ± 0.05	2.87 ± 0.05		
		Δ	2.71 ± 0.05	2.90 ± 0.05	1.01 ± 0.04	1.06 ± 0.04
[Ru(bpy) ₂ L ₂] ²⁺	racemic mixture	racemic mixture	2.69 ± 0.05	2.74 ± 0.05		
		Λ	2.62 ± 0.05	3.03 ± 0.05		
		Δ	2.76 ± 0.05	3.03 ± 0.05	1.01 ± 0.04	1.09 ± 0.04
[Ru(bpy) ₂ L ₃] ²⁺	racemic mixture	racemic mixture	2.72 ± 0.05	2.78 ± 0.05		
		Λ	2.29 ± 0.05	2.71 ± 0.05		
		Δ	2.73 ± 0.05	2.59 ± 0.05	1.00 ± 0.04	1.12 ± 0.04
			2.32 ± 0.05	2.55 ± 0.05		
			2.30 ± 0.05	2.28 ± 0.05		

by either racemic or Λ-[Ru(acac)₃] in a solution. The plots were expressed by the following equation:²⁷

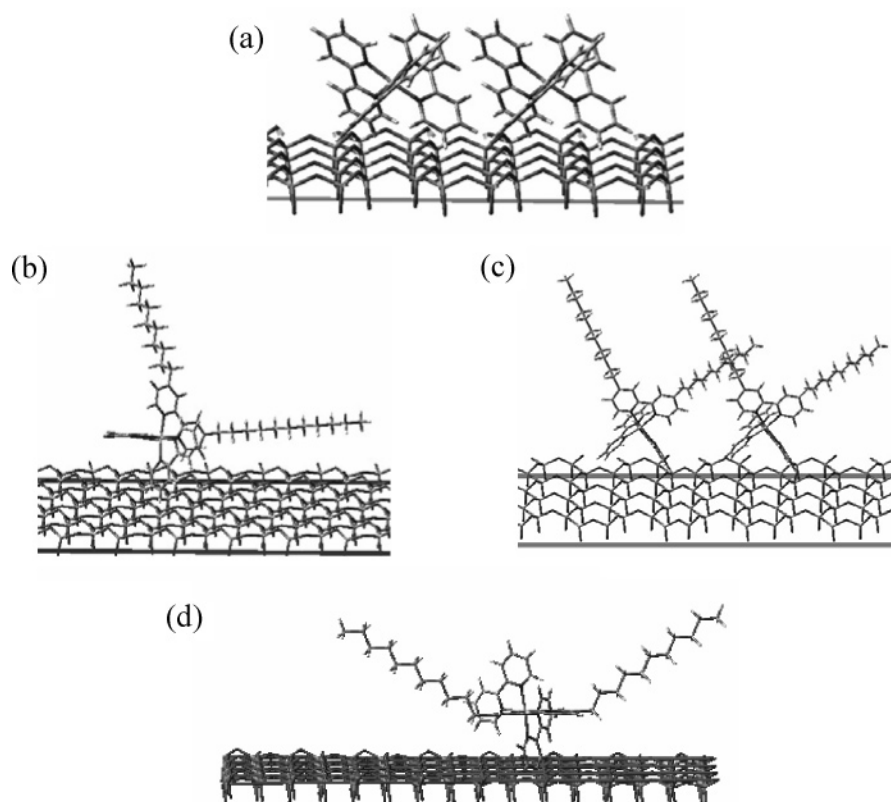
$$\frac{I_F}{I'_F} = 1 + \frac{k_q}{k_F}[q] \quad (3)$$

Here, I_F , I'_F , k_q , k_F , and $[q]$ are the phosphorescence intensity with and without a quencher, the bimolecular rate constant of quenching, the rate of spontaneous phosphorescence, and the concentration of quencher, respectively. From the slope of the plot, k_q/k_F was obtained. Table 2 summarizes the results when the fluorescence due to adsorbed racemic or Λ-[Ru(bpy)₂L_{*i*}]²⁺ (*i* = 1, 2, and 3) was quenched by racemic, or Δ- or Λ-[Ru(acac)₃]. The loading of an adsorbed chelate was taken to be 10 or 40% of the CEC of a clay. The ratio of k_q/k_F for Δ- and Λ-[Ru(acac)₃] as a quencher for excited Λ-[Ru(bpy)₂L_{*i*}]²⁺ was given in the last two columns of the table. Because k_F was identical between these two cases, the ratio gave the degree of

stereoselectivity in energy-transfer between adsorbed [Ru(bpy)₂L_{*i*}]²⁺ and [Ru(acac)₃] in a solution. According to them, at the loading of 10% of CEC, k_q/k_F was nearly equal between the Δ- and Λ-enantiomers of [Ru(acac)₃] within the experimental error (ca. 5%). Thus, no stereoselectivity appeared at this loading level for all three complexes. At the loading of 40% of CEC, however, there was a distinctive difference between the enantiomer of the quencher for all three kinds of Ru(II) chelates. In other words, Λ-[Ru(acac)₃] was more effective than Δ-[Ru(acac)₃] in quenching excited Λ-[Ru(bpy)₂L_{*i*}]²⁺ on a clay surface. Notably, such a stereochemical effect was largest for the case of [Ru(bpy)₂L₃]²⁺

Discussion

According to our previous reports, a racemic mixture of [Ru(phen)₃]²⁺ (phen = 1,10-phenanthroline) was adsorbed up to twice the excess of the CEC of a clay.⁵ Although [Ru(bpy)₂L₁]²⁺ belongs to the same tris-chelated complex and

SCHEME 1: Schematic Drawings Showing the Possible Orientation of Metal Complexes on a Clay Surface (a) [Ru(bpy)₂L₁]²⁺, (b) [Ru(bpy)₂L₂]²⁺ (Low Loading), (c) [Ru(bpy)₂L₂]²⁺ (High Loading), and (d) [Ru(bpy)₂L₃]²⁺

possesses nearly the same molecular size, the complex was found to be adsorbed to only 1.2 times the excess of the CEC for the enantiomeric case (Figure 1a). Racemic $[\text{Ru}(\text{bpy})_2\text{L}_1]^{2+}$ was adsorbed even to the smaller amount within the CEC. The main reason for the different maximum adsorption between these analogous chelates may be due to the fact that a phen ligand is bulkier and more hydrophobic than a bpy ligand so that $[\text{Ru}(\text{phen})_3]^{2+}$ has a much higher tendency for self-aggregation than $[\text{Ru}(\text{bpy})_2\text{L}_1]^{2+}$.²⁸ Our previous theoretical work suggested that such self-aggregation of cationic species on a clay surface was essential to achieving excess adsorption over the CEC.¹⁷ It resulted in the efficient screening of the negative charge of a clay layer so that an external anion was adsorbed to stabilize the excess adsorption layers of metal complexes.

A parameter dominating the intermolecular interaction among adsorbed molecules is the ratio of the sectional area of a molecule (S_m) to the surface area allotted to each adsorbate on a clay surface (S_c) or $f = S_m/S_c$. Statistically an adsorbed molecule is present as an isolated species for $f < 1$, whereas it is in contact with its neighbors for $f > 1$. When a divalent metal complex is adsorbed through an ion-exchange mechanism, S_c is calculated to be 1.82 nm^2 at the loading of 100% CEC on the basis of the elemental compositions (given in the Experimental Section).

Figure 6a–d shows the area occupied by $[\text{Ru}(\text{bpy})_2\text{L}_i]^{2+}$ on the basis of its theoretically obtained structure. For $[\text{Ru}(\text{bpy})_2\text{L}_1]^{2+}$, S_m was equated to the area of a circle projected by the molecule onto a clay surface. When the molecule is adsorbed with its C_3 axis perpendicularly, as already deduced from the electric dichroism measurements, the radius of the circle was estimated to be 0.52 nm , leading to $S_m = 0.85 \text{ nm}^2$. At the saturated adsorption (120% CEC in Figure 1), S_c is 1.52 nm^2 , leading to $f = 0.56$; that is, the molecules were adsorbed apart from their neighbors on an average. Despite this prediction, the stereochemical effects are seen at the loading well below 100 % CEC or the enantiomer is adsorbed more than the racemic mixture (Figure 1a). The results indicated that the molecules have a tendency to form an enantiomeric aggregate spontaneously under the intermolecular attractive force on a clay surface (Scheme 1a).

In the case of $[\text{Ru}(\text{bpy})_2\text{L}_2]^{2+}$, S_m is assumed to be equal to the area of a rectangle surrounding the base of a complex on a clay surface. Under this assumption, S_m depends on its orientation remarkably. We examine two extreme cases as shown in Scheme 1b and c. When one of its alkyl chains orients parallel to the surface (Scheme 1b), S_m is estimated to be 2.09 nm^2 (Figure 6b). When two alkyl chains are upright from a surface (Scheme 1c), S_m is estimated to be 1.47 nm^2 (Figure 6c). According to the electric dichroism results, the orientation of the chelate changed with the increase of loading. The orientation angle (θ) of the pseudo C_3 axis with respect to the normal of a clay surface is calculated to be 29° and 32° for the adsorbed states of Scheme 1b and c, respectively. These values are in agreement with the experimental results at 15 and 40% loading of CEC, respectively (Table 1). The XRD measurements also showed that the interlayer space ($d(001)$) was expanded with the increase of the adsorption amounts. The height of the adsorbed molecule is estimated to be 2 and 3 nm from Scheme 1b and c, respectively, which are again in agreement with the experimental results (Table 1). Thus, the complex was concluded to take the orientation as shown in Scheme 1c at the saturated adsorption (120% CEC). Under this orientation, S_m is estimated to be 1.47 nm^2 (Figure 6c). Because S_c is 1.52 nm^2 at 120% CEC, f is obtained to be 0.97 or the adsorbed molecules were

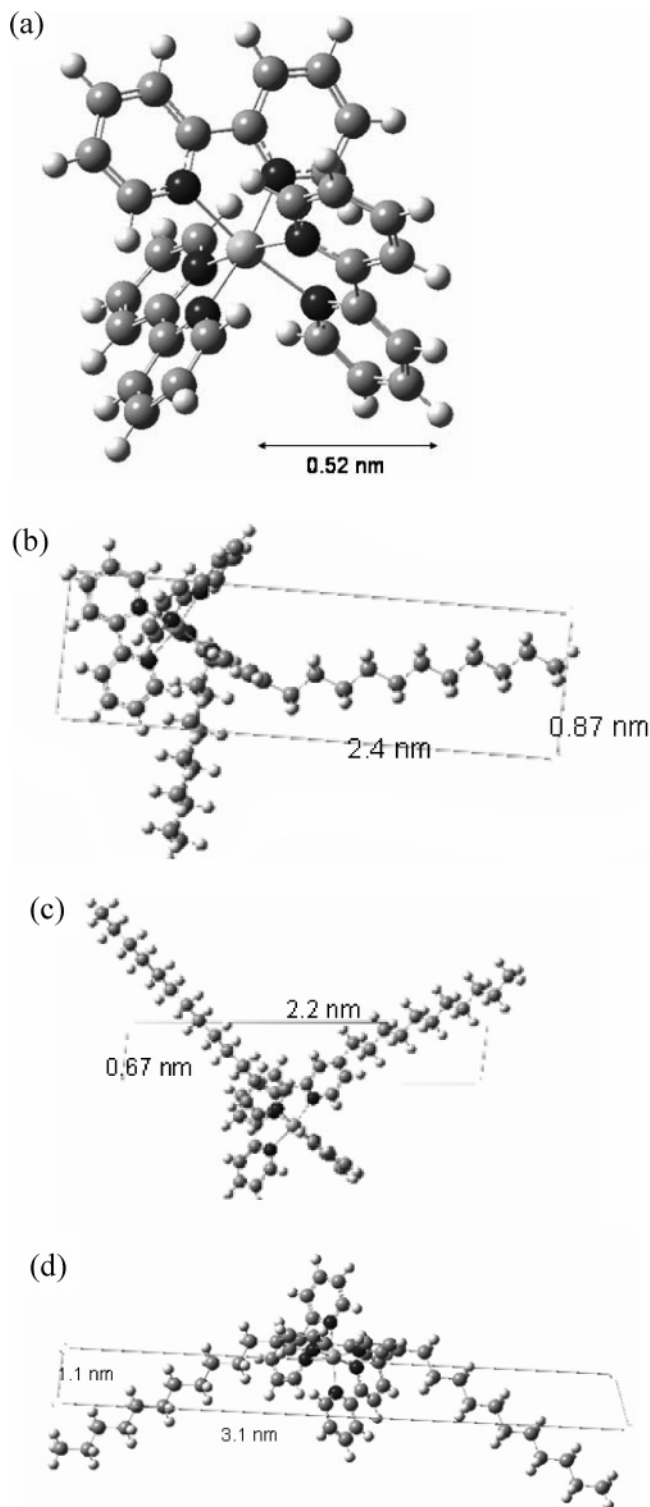


Figure 6. (a–d) Molecular structures and rectangular areas occupied by the metal complexes (a) $[\text{Ru}(\text{bpy})_2\text{L}_1]^{2+}$, (b) $[\text{Ru}(\text{bpy})_2\text{L}_2]^{2+}$ (low loading), (c) $[\text{Ru}(\text{bpy})_2\text{L}_2]^{2+}$ (high loading), and (d) $[\text{Ru}(\text{bpy})_2\text{L}_3]^{2+}$.

nearly in contact with each other. Thus, the observed stereochemical effect (Figure 2) is concluded to be caused by the configuration of the alkyl chains orienting upright from a surface.

$[\text{Ru}(\text{bpy})_2\text{L}_3]^{2+}$ is thought to take a unique orientation in its adsorption state or the two alkyl chains are parallel along a clay surface (Scheme 1d). The possibility of the normal orientation of these alkyl chains is low because the positive center of the molecule is too far from the clay surface. Under such a

configuration, θ and the basal spacing are calculated to be 20° and 3 nm, respectively. These are in agreement with the experimental observation. The S_m value of the molecule is calculated to be 3.41 nm² from Figure 6d. Because S_c is 2.02 nm² at 90% CEC (Figure 1c), f is obtained to be 1.69. It implies that the molecules were in contact with their neighbors, overlapping partially with each other. Such overlapping was thought to take place at the alkyl chain regions but not at the bpy ligands. Therefore, no stereochemical effect was observed in the adsorbed states (Figure 1c).

Energy transfer from excited $[\text{Ru}(\text{bpy})_2\text{L}_i]^{2+}$ to $[\text{Ru}(\text{acac})_3]$ is known to take place by the electron-transfer mechanism, in which an electron jumps from excited $[\text{Ru}(\text{bpy})_2\text{L}_i]^{2+}$ to $[\text{Ru}(\text{acac})_3]$.^{29,30} Because these two reactants should be in contact with each other for the occurrence of such electron jumping, stereoselectivity is expected to arise from the stacking effect of the ligands between two reacting metal complexes. In such a case, the direction that the ligands of the adsorbed complex are oriented on the clay surface is of vital importance.

Comparing the adsorbed states among three investigated molecules (Scheme 1), it is suspected that chiral discrimination between adsorbed $[\text{Ru}(\text{bpy})_2\text{L}_3]^{2+}$ and incoming $[\text{Ru}(\text{acac})_3]$ is performed by the stacking interaction of the two bpy and acac ligands. The helically twisted bpy ligands of $[\text{Ru}(\text{bpy})_2\text{L}_3]^{2+}$ stack well with the acac ligands of $[\text{Ru}(\text{acac})_3]$ when the latter approaches the former with their C_3 axes in parallel. Stacking is more efficient for the Λ – Λ pair rather than the Λ – Δ pair. In fact, the Λ – Λ pair gives more efficient electron transfer than the Λ – Δ pair as given in Table 1. As summarized in Table 2, the highest discrimination was achieved for the case of $[\text{Ru}(\text{bpy})_2\text{L}_3]^{2+}$ at maximum loading. Such a chiral discrimination site is most effective in this case because the two bpy ligands are oriented in the outward direction. In this way, orientation tuning has been attempted to achieve high discrimination capability.

In the field of photochemical reactions, there have been a number of examples demonstrating the importance of steric constraint by a clay surface for the achievement of stereoregularity.^{13,31} In contrast to these examples, the present work is unique in realizing the achievement of stereoselectivity for the reactions between an adsorbed species and a reactant in a homogeneous solution.

Conclusions

In the present study, the tuning of orientation was performed by attaching alkyl chains at different positions of a bpy ligand of a metal complex adsorbed by a clay. As a result, the chiral discrimination was performed toward energy-transfer reactions. Stereoselectivity appeared most when $[\text{Ru}(\text{bpy})_2\text{L}_3]^{2+}$ oriented with its two helically twisted bpy ligands projected toward a homogeneous medium.

Acknowledgment. This work has been financially supported by a Grant-in-Aid for Scientific Research on Priority Areas (417) from the Ministry of Education, Culture, Sports, Science and Technology (MEXT) of Japanese Government. Thanks are due to Professor Sasai (Nagoya University) for his valuable discussion in interpreting electric dichroism results.

References and Notes

(1) *Nanoparticles and Nanostructured Films: Preparation, Characterization and Applications*; Fendler, J. H., Ed.; Weinheim: New York, 1998.

- (2) Liu, Y.; Pinnavaia, T. J. *J. Am. Chem. Soc.* **2003**, *125*, 2377.
- (3) Ogawa, M.; Kuroda, K. *Chem. Rev.* **1989**, *89*, 1359.
- (4) Gosh, P. K.; Bard, A. J. *J. Phys. Chem.* **1984**, *88*, 5519.
- (5) (a) Yamagishi, A. *J. Am. Chem. Soc.* **1985**, *107*, 732. (b) Yamagishi, A. *Coord. Chem. Rev.* **1987**, *16*, 131 and references therein.
- (6) Villumure, G. *Clays Clay Miner.* **1990**, *38*, 622.
- (7) Breu, J.; Raj, N.; Catlow, R. A. *J. Chem. Dalton Trans.* **1999**, *6*, 835.
- (8) Wakabayashi, N.; Nishimura, S.; Kakegawa, N.; Sato, H.; Yamagishi, A. *Clay Sci.* **2004**, *12*, 259.
- (9) He, J. X.; Sato, H.; Umemura, Y.; Yamagishi, A. *J. Phys. Chem. B* **2005**, *109*, 4679.
- (10) (a) Takagi, S.; Tryk, D. A.; Inoue, H. *J. Phys. Chem. B* **2002**, *106*, 5455. (b) Eguchi, S.; Takagi, S.; Tachibana, H.; Inoue, H. *J. Phys. Chem. Solids* **2004**, *65*, 403. (c) Takagi, S.; Shimada, M.; Eguchi, M.; Yui, T.; Yoshida, H.; Tryk, D. A.; Inoue, H. *Langmuir* **2002**, *18*, 2265.
- (11) Choy, J.-H.; Yoon, J.-B.; Jung, H. *J. Phys. Chem. B* **2002**, *106*, 11120.
- (12) Umemura, Y.; Yamagishi, A.; Schoonheydt, R.; Persoons, A.; Schryver, F. *J. Am. Chem. Soc.* **2001**, *17*, 992.
- (13) (a) Ito, T.; Shichi, T.; Yui, T.; Takahashi, H.; Inui, Y.; Takagi, K. *J. Phys. Chem. B* **2005**, *109*, 3199. (b) Ito, T.; Shichi, T.; Yui, T.; Takagi, K. *Langmuir* **2005**, *21*, 3217. (c) Zhang, G.; Yui, T.; Shichi, T.; Takagi, K. *Compos. Interfaces* **2004**, *11*, 307. (d) Ohtani, O.; Itoh, T.; Monna, Y.; Sasai, R.; Shichi, T.; Yui, T.; Takagi, K. *Bull. Chem. Soc. Jpn.* **2005**, *78*, 698.
- (14) Sakai, N.; Ebina, Y.; Takada, K.; Sasaki, T. *J. Am. Chem. Soc.* **2004**, *126*, 5851.
- (15) Saruwatari, K.; Sato, H.; Idei, T.; Kameda, J.; Yamagishi, A.; Takagaki, A.; Domen, K. *J. Phys. Chem. B* **2005**, *109*, 12410.
- (16) Mallouk, T. E.; Gavin, J. A. *Acc. Chem. Res.* **1998**, *31*, 209.
- (17) (a) Sato, H.; Yamagishi, A.; Kato, S. *J. Am. Chem. Soc.* **1992**, *114*, 10933. (b) Sato, H.; Yamagishi, A.; Naka, K.; Kato, S. *J. Phys. Chem.* **1996**, *100*, 1711.
- (18) Umemura, Y.; Shinohara, E. *Chem. Commun.* **2004**, 1110.
- (19) Breu, J.; Stoll, A.; Lange, K. G.; Probst, T. *Phys. Chem. Chem. Phys.* **2001**, *3*, 1232.
- (20) Tamura, K.; Sato, H.; Yamashita, S.; Yamagishi, A.; Yamada, H. *J. Phys. Chem. B* **2004**, *108*, 8287.
- (21) (a) Naka, K.; Sato, H.; Fujita, T.; Iyi, N.; Yamagishi, A. *J. Phys. Chem. B* **2003**, *107*, 8469. (b) Taniguchi, M.; Kaneyoshi, M.; Nakamura, Y.; Yamagishi, A.; Iwamoto, T. *J. Phys. Chem.* **1990**, *94*, 5896.
- (22) Sato, H.; Hiroe, Y.; Sasaki, T.; Ono, K.; Yamagishi, A. *J. Phys. Chem. B* **2004**, *108*, 17306.
- (23) Yamagishi, A.; Taniguchi, M.; Takahashi, M.; Asada, C.; Matsushita, N.; Sato, H. *J. Phys. Chem.* **1994**, *98*, 7555.
- (24) Dourlent, M.; Hogrel, J. F.; Helen, C. *J. Am. Chem. Soc.* **1974**, *96*, 3398.
- (25) Frisch, M. J.; Trucks, G. W.; Schlegel, H. B.; Scuseria, G. E.; Robb, M. A.; Cheeseman, J. R.; Montgomery, J. A., Jr.; Vreven, T.; Kudin, K. N.; Burant, J. C.; Millam, J. M.; Iyengar, S. S.; Tomasi, J.; Barone, V.; Mennucci, B.; Cossi, M.; Scalmani, G.; Rega, N.; Petersson, G. A.; Nakatsuji, H.; Hada, M.; Ehara, M.; Toyota, K.; Fukuda, R.; Hasegawa, J.; Ishida, M.; Nakajima, T.; Honda, Y.; Kitao, O.; Nakai, H.; Klene, M.; Li, X.; Knox, J. E.; Hratchian, H. P.; Cross, J. B.; Bakken, V.; Adamo, C.; Jaramillo, J.; Gomperts, R.; Stratmann, R. E.; Yazyev, O.; Austin, A. J.; Cammi, R.; Pomelli, C.; Ochterski, J. W.; Ayala, P. Y.; Morokuma, K.; Voth, G. A.; Salvador, P.; Dannenberg, J. J.; Zakrzewski, V. G.; Dapprich, S.; Daniels, A. D.; Strain, M. C.; Farkas, O.; Malick, D. K.; Rabuck, A. D.; Raghavachari, K.; Foresman, J. B.; Ortiz, J. V.; Cui, Q.; Baboul, A. G.; Clifford, S.; Cioslowski, J.; Stefanov, B. B.; Liu, G.; Liashenko, A.; Piskorz, P.; Komaromi, I.; Martin, R. L.; Fox, D. J.; Keith, T.; Al-Laham, M. A.; Peng, C. Y.; Nanayakkara, A.; Challacombe, M.; Gill, P. M. W.; Johnson, B.; Chen, W.; Wong, M. W.; Gonzalez, C.; Pople, J. A. *Gaussian 03*, revision C.02; Gaussian, Inc.: Wallingford, CT, 2004.
- (26) Taniguchi, M.; Yamagishi, A.; Iwamoto, T. *Inorg. Chem.* **1991**, *30*, 2462.
- (27) Stern, O.; Volmer, M. *Phys. Z.* **1919**, *20*, 183.
- (28) Masuda, Y.; Yamatera, H. *Bull. Chem. Soc. Jpn.* **1984**, *57*, 58.
- (29) Inukai, K.; Hotta, Y.; Tomura, S.; Takahashi, M.; Yamagishi, A. *Langmuir* **2000**, *16*, 7679.
- (30) Ohkubo, K.; Hamada, T.; Ishida, H.; Fukushima, M.; Watanabe, M. *J. Mol. Catal.* **1994**, *89*, L5.
- (31) Thomas, J. K. *Acc. Chem. Res.* **1988**, *21*, 275.